Consequences of a noncovariant description of slow and fast protons from *p*-C, C-C, and C-Ta interactions at 3.3*A* GeV

Khaled Abdel-Waged*
Physics Department, Faculty of Applied Science, Umm Al-Qura University, Unit 126, P.O. Box 7047, Saudi Arabia
(Received 20 July 2002; published 10 February 2003)

A comparison is made between a typical intranuclear cascade (INC) model and the experimental inclusive slow ($T<0.4$ GeV) and fast ($T>0.4$ GeV) proton spectra in the *p*-C, C-C, and C-Ta in interactions at 3.3*A* GeV over a broad angular interval from 0° to 180°. It is found that the INC model reproduces rather well the inclusive slow and fast proton spectra, provided that the mean number of interacting protons (participants) in the corresponding angular interval does not exceed 2. The systematic discrepancies are identified and shown to correspond mainly to the noncovariant nature of the INC calculations.

DOI: 10.1103/PhysRevC.67.024901 PACS number(s): 25.75.−q, 24.10.Lx, 25.40.Ve

I. INTRODUCTION

Light/heavy-ion collisions at intermediate energies (between a few MeV/nucleon to a few GeV/nucleon) are expected to reveal various aspects of the hadronic many-body problem.

An early, simple, and successful attempt for describing nucleus-nucleus (AA) collisions at intermediate energies has been the intranuclear cascade (INC) model [1–4], where the reaction is simulated by a sequence of individual nucleon-nucleon (NN) scatterings between nucleons. A lot of experimental data at 1–4*A* GeV were well explained by such a model, however, a systematic disagreement is found when the degree, to which nuclei are destroyed is significant [5–9].

Possible causes are the absence of mean field and/or the manifest Poincare covariance of the dynamics. Such effects, although pointed out in Refs. [5,6,10–13] have not practically been tested. Therefore, in order to investigate these effects, we perform here a systematic comparison of the INC results with those of the relativistic quantum molecular dynamics (RQMD) model [14]. The latter includes, in addition to the NN scatterings, both the mean field as well as the features of the Lorentz covariance of a system of interacting particles. (Note that, although the kinematics are relativistic in the INC, the interactions are treated nonrelativistically, which breaks the Lorentz covariance of the theory.)

To ensure that the effects discussed here are not sensitive to model parameters, such as the different equation of states and the modified NN cross sections, we shall concentrate, as in Ref. [15], on the inclusive proton spectra. More specifically, we are going to compare the INC and RQMD results with the experimental [16,17], inclusive cross sections of the proton yield as a function of the kinetic energy (T) at fixed angles from 0° to 180° for *p*-C, C-C, and C-Ta interactions at 3.3*A* GeV.

The paper is organized as follows: Section II deals with a brief introduction to the formalism used in the INC and RQMD models. The results are presented in Sec. III and finally we summarize our findings in Sec. IV.

II. DESCRIPTION OF THE BASIC MODELS

A. The intranuclear cascade model

In this section, we outline the basic ideas of the INC model and summarize the most important features.

(i) Initially, the nucleons of the two colliding nuclei that have mass numbers A and B are ascribed the coordinates (x_i, y_i, and z_i, where $1\leqslant i\leqslant A$) and (x_j, y_j, and z_j, where $1\leqslant j\leqslant B$) in the rest frames of the corresponding nuclei. The Wood-Saxon density is used for nuclei with A, $B\geqslant 10$, with parameters $R_A=1.07A^{1/3}$ fm and $c=0.545$ fm. In choosing the nucleon coordinates, the nucleon core is included (no two nucleons can be closer than $2R_c$, $R_c=0.4$ fm). In each nucleus, the nucleon momenta are sampled according to zero-temperature Fermi distributions. The maximum allowed Fermi momenta of nucleons are given by

$$P_F=\hbar[3\pi^2\rho(r)]^{1/3}, \tag{1}$$

where $\rho(r)$ is the nuclear density.

(ii) Taking into account the Lorentz contraction of the projectile nucleus A, the coordinates z_i in the rest frame of the target nucleus B are written as $z_i\rightarrow z_i/\gamma-R_A/\gamma-R_B$, where γ is the Lorentz factor of the projectile nucleus, and R_A and R_B are the radii of the nuclei involved.

(iii) All nucleons are allowed to move freely (e.g., along straight lines) with their respective momenta until the relative distance for one of the pairs (i, j) has reached a minimum,

$$d_{min}\leqslant\sqrt{\sigma_{tot}/\pi}, \tag{2}$$

where $d_{min}=\sqrt{(b_x+x_i-x_j)^2+(b_y+y_i-y_j)^2}$ is defined in the three-dimensional configuration space. $b_{x,y}$ and σ_{tot} are the components of the impact parameter vector and the total NN cross section, respectively. In the rest frame of the target nucleus, the time of possible interactions is $t_{i,j}=(z_j-z_i)/v$, where v is the speed of the projectile nucleus.

*Permanent address: Physics Department, Faculty of Science, Benha University, Egypt.

 ©2003 The American Physical Society

(iv) A nucleon involved in the interaction is treated as a cascade particle as soon as it undergoes its first interaction. After the first NN collision has been completed, the time is increased by $t_{i,j}$ so that $z_k \rightarrow z_k + v t_{i,j}$. The possible interactions of cascade particles with the nucleons of the target and projectile nuclei are considered next. The time of possible interactions is given by

$$t_{i(j),k} = \frac{(\mathbf{r}_{i(j),k} \cdot \mathbf{v}_k)}{|v_k|^2}, \tag{3}$$

where $\mathbf{r}_{i(j),k} = \mathbf{r}_{i(j)} - \mathbf{r}_k$, $\mathbf{r}_k$ and $\mathbf{v}_k$ are the radius and velocity vectors of the kth cascade particle, respectively. Of all possible interactions, the one that is closest in time to the preceding interaction is chosen. The sequence of two-body collisions is followed until the number of all possible interactions is exhausted, which is possible once the nuclei diverge or once all cascade particles escape from the nuclei.

(v) At each collision, the final momenta are randomly selected taking into account the experimental differential NN cross section with total energy and momentum conserved.

(vi) Following the completion of the cascade process, the masses of the residual nuclei are determined by product nucleons that have not escaped from the nuclei and nucleons that belong to the nuclei A and B, but which have not been involved in interaction.

In addition to this picture, several features are added. First, pion production is introduced by considering the inelastic NN cross section. Second, the Pauli principle and the energy-momentum conservation are obeyed in each intranucleon interaction. Third, the interdependence of projectile and target cascades is achieved through local correlations of density of nucleons from colliding nuclei, which result from intranuclear collisions

The parameters of the INC model were determined as a result of an analysis of hadron-nucleus (hA) interactions [18,19]. We do not change these values in our calculations. The remaining details of the model can be found in Ref. [5].

It should be noted here that the above model is recognized as the best model applied for smaller projectile interactions with heavy nuclei in the intermediate energy range ($1A$–$10A$ GeV) [20,21].

B. The relativistic quantum molecular dynamics model

In contrast to the INC model, the phase space in the RQMD model is enlarged to $8N$ dimensions [the positions $q_i = (\mathbf{r}_i, t)$ and momenta $p_i = (E_i, \mathbf{p}_i)$ of the N particles as four-vectors] [14]. The equations of motion are defined by the Poincare covariant mass shell constraints and the time fixations. The on-mass shell constraints are given by

$$H_i = p_i^2 - m_i^2 - \tilde{V}_i = 0, \quad i = 1,2,\ldots,N, \tag{4}$$

where m_i and $\tilde{V}_i$ are the mass and the Lorentz scalar quasipotential for the ith nucleon, respectively. Equation (4) defines the effective baryon masses in a medium and simulates the effect of the mean fields.

The argument of the potential is taken as the Lorentz invariant squared transverse distance

$$q_{Tij}^2 = q_{ij}^2 - \frac{(q_{ij} p_{ij})^2}{p_{ij}^2}, \tag{5}$$

with $q_{ij} = q_i - q_j$ being the four-dimensional distance and $p_{ij} = p_i + p_j$ the sum of the momenta of the two interacting particles i and j. q_{Tij} is defined in a way that the squared covariant transverse distance q_{Tij}^2 reduces to the usual squared distance r_{ij}^2 in the c.m. system of the two particles i and j.

After having fixed the particle energies by the mass shell constraints, the relative time of the particles are also fixed by $N-1$ independent Poincare invariant time fixations,

$$\chi_i = \sum_{j \neq i} \frac{e^{q_{ij}^2/L_c}}{q_{ij}^2/L_c} q_{ij} p_{ij} = 0, \quad i = 1,2,\ldots,N-1, \tag{6}$$

with $L_c = 8.66$ fm^2. Under these time fixations, the two colliding particles have equal values of their time coordinates in their c.m. frame in the dilute gas limit.

An Nth constraint relates the time of the particles to the time evolution parameter τ,

$$\chi_N = \hat{p} Q - \tau = 0, \tag{7}$$

with $\hat{p} = p/\sqrt{p^2}$, $p = \Sigma_i p_i$, $Q = 1/N \Sigma_i q_i$. The Hamiltonian is a linear combination of the Poincare invariant constraints,

$$H = \sum_{i=1}^{N} \lambda_i H_i + \sum_{i=1}^{N-1} \lambda_{N+i} \chi_i, \tag{8}$$

where the Lagrange multipliers λ_i are determined by the fact that the complete set of $2N$ constraints must be fulfilled during the whole time evolutions. The Hamiltonian (8) generates the equation of motion,

$$\frac{dq_j}{d\tau} = \frac{\partial H}{\partial p_j} = 2\lambda_j p_j - \sum_{i=l}^{N} \lambda_i \frac{\partial \hat{V}_i}{\partial p_j}, \quad j = 1,\ldots,N,$$

$$\frac{dp_j}{d\tau} = -\frac{\partial H}{\partial q_j} = \sum_{i=1}^{N} \lambda_i \frac{\partial \hat{V}_i}{\partial q_j}, \quad j = 1,\ldots,N. \tag{9}$$

In Eq. (9), it is assumed that the time fixations (6) do not affect the particle motion. The equations of motion (9) are assumed to propagate the baryon during the reaction. The baryonic interaction by quasipotentials reflects the soft part of the baryon interaction in nuclear matter. If the quasipotentials are set to zero, one recovers the free motion with the correct relativistic kinematics as solutions of the equations of motion. The propagation is combined with the quantum effects such as stochastic scattering and the Pauli blocking in a similar manner as in the INC. In the RQMD, however, the collision part is treated in a covariant fashion. Therefore, all quantities which determine the collision must be Lorentz invariant. In the RQMD, two baryons are allowed to collide if their distance

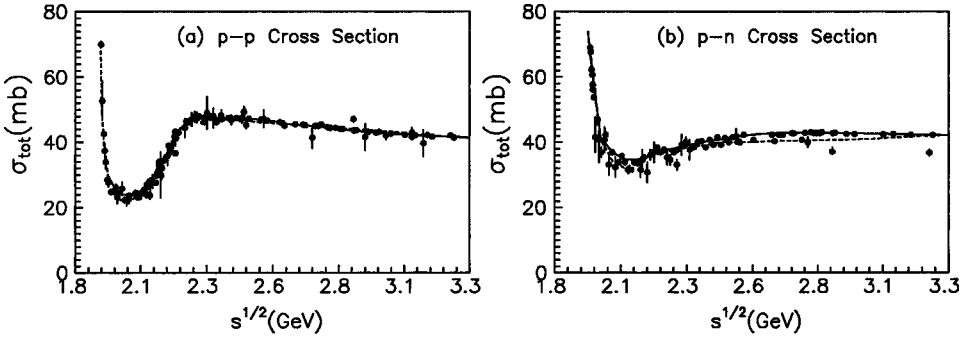

FIG. 1. The fitted p-p (a) and p-n (b) total cross sections that are used by the RQMD (solid lines) and INC (small dashed lines) models together with measured data (closed circles with error bars) taken from particle data group Ref. [22].

$$\sqrt{-q_{Tij}^2} \leqslant \sqrt{\frac{\sigma_{tot}(s^1/2)}{\pi}}. \tag{10}$$

where $\sigma_{tot}(\sqrt{s})$ is the total NN cross section at a given c.m. energy of the colliding nucleon system.

In order to compare the RQMD and INC models precisely, it is necessary to perform a comparison between the experimental total cross sections and that used in the two programs [Eqs. (2) and (10)]. In Fig. 1, we show the p-p (a) and p-n (b) total cross sections parametrized by the RQMD (solid) and INC (small dashed) models. In the same, figure we show the corresponding experimental total cross sections with error bars [22]. For the p-p case, both parametrizations are identical and well fits the data for the whole energy range. On the other hand, for the p-n case, the RQMD parametrization slightly overestimates the INC one, in the region $2.3 < \sqrt{s} < 3.1$, but both are essentially the same as the data.

In the numerical calculations, the RQMD (version 2.4) is running in two modes, the cascade mode (RQMD/C) and the one that includes the mean field effects (RQMD/M). In both modes, only options common to the features of the INC model are switched on. For example, the initial nuclei are chosen to be of a Wood-Saxon type. The maximum allowed Fermi momentum is computed according to Eq. (1). The decay processes of resonances with masses higher than 2 GeV are neglected. Finally, pion absorption is taken into account. Thus, the differences observed in the final results of the RQMD/C and INC calculations are regarded as evidence of the Lorentz covariance effects.

III. RESULTS AND DISCUSSION

In this section, we compare the proton spectra predicted by the RQMD/C, RQMD/M, and INC simulations for p-C, C-C, and C-Ta collisions at 3.3A GeV. The impact parameter for the calculated p-C and C-C interactions have been selected from $0 \leqslant b \leqslant 2$ fm. For the calculated C-Ta interactions, it is $0 \leqslant b \leqslant 3$ fm. The data used in the present comparison are from the survey papers of Refs. [16,17]. As was done for the experimental data, the analysis of the RQMD/C, RQMD/M, and INC generated events exclude single-charged fragments with $p > 3$ GeV/c.

In order to study the effect of the mean field on the proton spectra, we compare, in Fig. 2, both the RQMD/C and RQMD/M with the whole experimental proton spectra for p-C, C-C, and C-Ta (at 3.3A GeV) interactions as a function of the kinetic energy of proton (T) in various angular intervals from $\theta = 0°$ to 180°. The data presented here are the combination of the slow proton spectra with $0.05 \leqslant T \leqslant 0.4$ GeV at fixed angles from $\theta = 0°$ to 180° [16] and the fast proton spectra with $T > 0.4$ GeV at angles from $\theta = 0°$ to 90° [17]. The RQMD/M sample is calculated with the repulsive part of the quasipotential (a Skyrme-type interaction is used with parameters $\alpha = -0.4356$ GeV, $\beta = 0.385$ GeV, and $\gamma = 7/6$) acting between baryons only, i.e., with the δ-δ and nucleon-baryon attractions turned off. This gives, as explained in Ref. [21], a strong repulsion at high densities.

Let us first focus on the proton spectra of slow protons with kinetic energies from 0.05 to 0.4 GeV at fixed angles over the range $\theta = 0°$ to 180°. This range of proton energies is selected to bring out the comparison between both the RQMD/C and RQMD/M calculations and the data in the target fragmentation region. As one can see, both the RQMD/C (small dashed histograms) and RQMD/M (solid histograms) can nicely predict the experimental behavior: a monotonic decrease of the proton spectra for p-C and C-C interactions from 0.05 to 0.4 GeV in angular intervals up to 50°. Starting at 50°, the spectra fall rapidly as the kinetic energy increases. For C-Ta interactions, both the calculated and experimental spectra of protons fall off sharply to 0.2 GeV and then flattens out in all angular intervals.

Let us now proceed to the spectra of fast protons with kinetic energy above 0.4 GeV in the angular interval from $\theta = 0°$ to 90°. The group of protons with $T > 0.4$ GeV includes protons produced by the fragmentation of the projectile nucleus and protons from the central rapidity region, that can include protons from the fragmentation of the target nucleus that have acquired a large momentum transfer as well as protons produced by the fragmentation of the projectile nucleus and retarded in the target. As one can see that the results of the two different RQMD calculations for the fast proton spectra agree with the corresponding experimental data for the studied reactions in the corresponding energy and angular ranges. Nevertheless, systematic discrepancies appear for C-Ta interactions, the different RQMD spectra fall off more steeply with T than do the experimental data in the angular range from $\theta = 10°$ to 70°.

The systematic difference between the RQMD predictions and the data for C-Ta interactions are better shown in Table I, where we compare the values of the experimental fitted inverse slope parameters T_B as a function of the specified an-

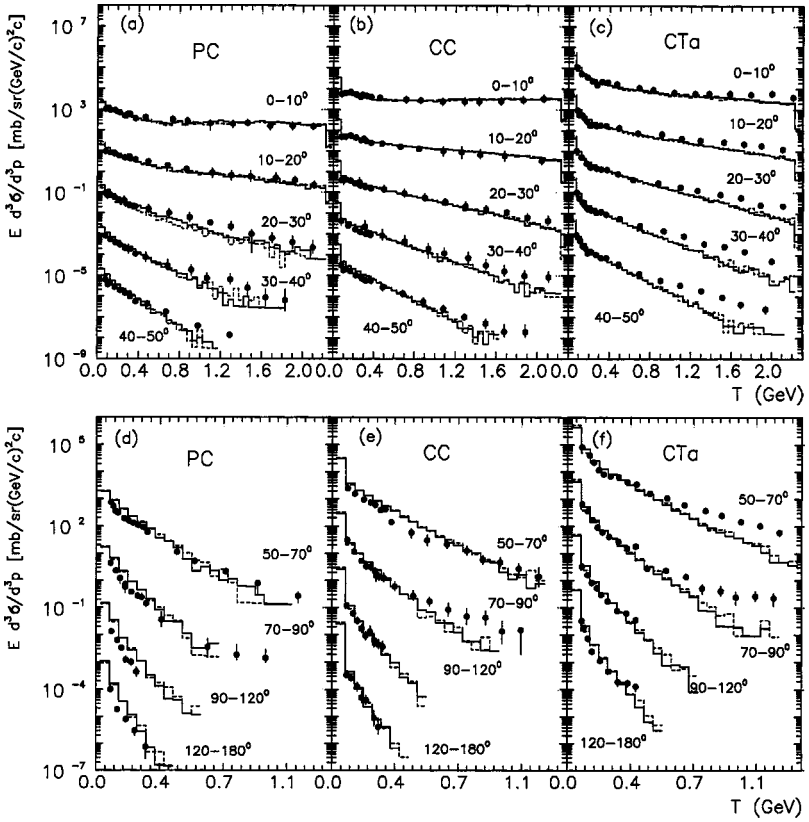

FIG. 2. The experimental (error bars) proton inclusive cross section as a function of proton kinetic energy (T) for p-C, C-C, and C-Ta interactions at 3.3A GeV in the angular range from 0° to 180°, as compared to the RQMD/M (solid histograms) and RQMD/C (small dashed histograms) calculations. In order to avoid superposition of curves, only the histograms and the data for the smallest angle in both the upper [(a), (b,) and (c)] and lower [(d), (e), and (f)] panels, are given in absolute value. The other ones have been multiplied by $10^{-2}, 10^{-4}, \ldots$ for other angles in increasing order.

gular intervals with the corresponding RQMD values [T_B is extracted from the fitting of the invariant cross section $Ed^3\sigma/d^3p$ with an exponential function $A\exp(-T/T_B)$, where A is a normalization factor]. At each angular interval for slow and fast protons, the calculated spectra were fitted over the range covered by the experimental data. As one can see from the table, the slopes of T_B of slow and fast RQMD protons spectra depend on the quasipotentials acting between baryons used in the calculations. The calculation that produced the RQMD/M sample for slow proton spectra yields smaller inverse slope parameters which gives results in much better agreement with the data for C-Ta interactions in all the angular intervals. This may imply that without the Lorentz covariance of the mean field, we can not correctly describe the intrinsic motion of nucleons, which is relatively low energy phenomena in the fast moving nuclei. As for the fast

TABLE I. Values of the parameter T_B found by approximation of both the calculated and experimental spectra of slow (top) and fast (bottom) protons in the C-Ta interactions at 3.3A GeV.

$\Delta\theta$°	ΔT (GeV)	T_B(Expt.) (GeV)	T_B(RQMD/M) (GeV)	T_B(RQMD/C) (GeV)
Slow proton spectra				
10−20	0.075−0.275	0.119±0.006	0.127	0.151
20−30	0.075−0.275	0.118±0.004	0.118	0.136
30−40	0.075−0.275	0.105±0.003	0.107	0.127
40−50	0.075−0.222	0.086±0.003	0.088	0.107
50−70	0.075−0.222	0.064±0.004	0.075	0.089
70−90	0.075−0.222	0.055±0.004	0.062	0.069
90−120	0.075−0.222	0.050±0.002	0.052	0.059
120−180	0.075−0.222	0.044±0.001	0.043	0.051
Fast proton spectra				
10−20	0.4−2.6	0.725±0.015	0.523	0.562
20−30	0.4−2.6	0.446±0.011	0.322	0.344
30−40	0.4−1.5	0.313±0.011	0.231	0.233
40−50	0.4−1.1	0.262±0.011	0.175	0.177
50−70	0.4−1.0	0.200±0.011	0.128	0.135
70−90	0.4−0.9	0.193±0.028	0.086	0.098

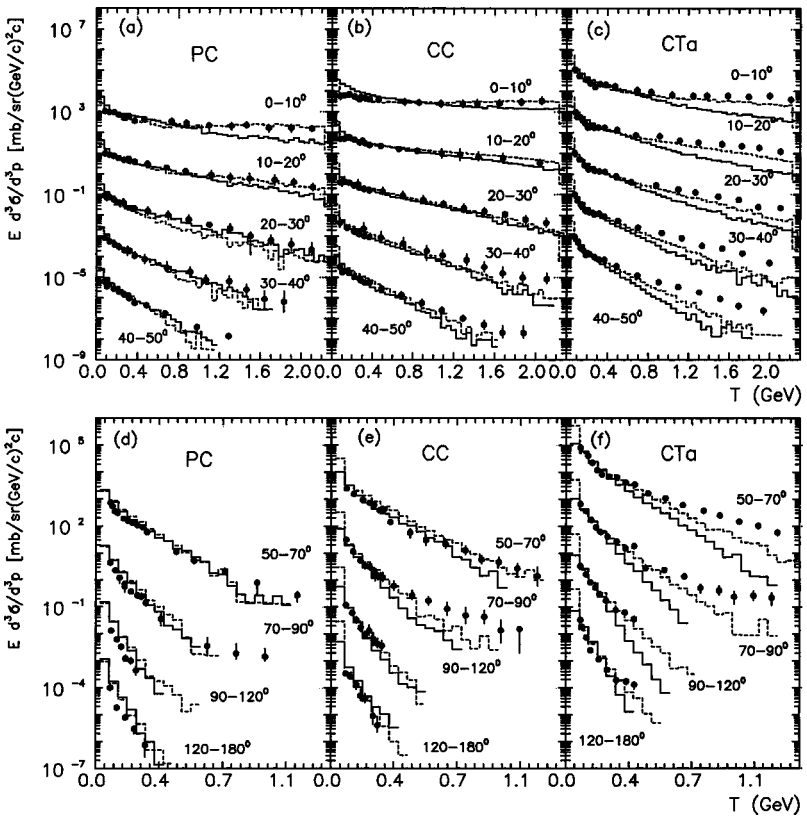

FIG. 3. Same as Fig. 2, but here the solid and small dashed histograms denote the RQMD/*C* and the INC calculations, respectively.

proton spectra, both the RQMD/*M* and RQMD/*C* results always underpredict the observed T_B values, while the RQMD/*C* results yield a slightly larger T_B values.

It should be noted that, in Refs. [23,24], the RQMD model is shown to underestimate the proton spectra in the midrapidity region for Si+Au at 15*A* GeV/*c* and Au+Au at 11.5*A* GeV/*c*. The final proton spectra for the latter reactions is found to be insensitive to dense matter effects, for instance, pion absorption, repulsive mean field, and modified cross sections. This may suggest that the central region in *AA* collisions at $3A-15A$ GeV/*c* cannot be explained by simple superpositions of *NN* collisions.

In Fig. 3, we investigate the noninvariance effects by comparing both the RQMD/*C* and INC simulations with the experimental proton invariant cross sections for the studied interactions. As one can see, the INC calculations are in agreement with both the RQMD/*C* and the data for *p*-C and C-C interactions. Only at $0°-10°$, the INC predicts a slight (large) excess of slow proton spectra ($T<0.4$ GeV) for *p*-C (C-C) interactions. At higher energies ($T>0.9$ GeV), the observed pattern is reversed, where the RQMD/*C* (and the data) spectra of fast protons are harder than those of the INC. As for the C-Ta interactions, the INC spectra fall off more steeply with *T* than do the RQMD/*C* (and the data) in the angular range from $\theta=0°$ to $\theta=90°$, though at larger angles, the INC results are in a good agreement with the RQMD/*C* (and the data).

A systematic difference between the RQMD/*C* and INC calculations is observed for C-C and C-Ta interactions at very slow proton energies ($T\leqslant 50$ MeV), especially at large angles (see Fig. 3). This difference is due to the clusterization effect, which is inherited in the INC and disregarded by the RQMD calculations. This may indicate that the clusterization effect plays an insignificant role for the calculated energy spectra of the reactions considered above $T=50$ MeV.

It should be noted that, a two step model based on the QMD model (DQMD) [10] is used to analyze these data. Calculations with the DQMD model yield almost the same results as the INC. This may imply that the invaraint inclusive proton spectra are insensitive to model parameters.

Finally, let us look for the effect of a covariant treatment on the number of participant protons for the specified interactions. This is done in Fig. 4. Here, the angular interval dependence on the mean number of participant protons $\langle N_p\rangle$ is shown by using the RQMD/*C*, RQMD/*M*, and INC simulations. The number of participant protons is defined as protons with momentum $0.3<p<3$ GeV/*c* and $\theta>4°$ [25,26]. This number is used in Refs. [25,26] to measure the degree of centrality for the reactions under study. It is shown from Fig. 4 that, for asymmetric (*p*-C and C-Ta) collisions, the $\langle N_p\rangle$ increases with increasing θ reaching a maximum at $50°-70°$ and then decreases. As for symmetric (C-C) collisions, the $\langle N_p\rangle$ has a maximum at $10°-20°$, decreases with increasing θ and then approaches a constant value at $>70°-90°$. The $\langle N_p\rangle$ is larger in the most forward than in the most backward angles for *p*-C and C-C interactions, whereas it is nearly the same for C-Ta interactions.

It is interesting to see that the RQMD/*M* shows more $\langle N_p\rangle$ than the RQMD/*C*. This is due to the fact that, with potentials on, the particles feel some kind of repulsion, especially, in the compressed central zone ($\Delta\theta=50°-70°$ for

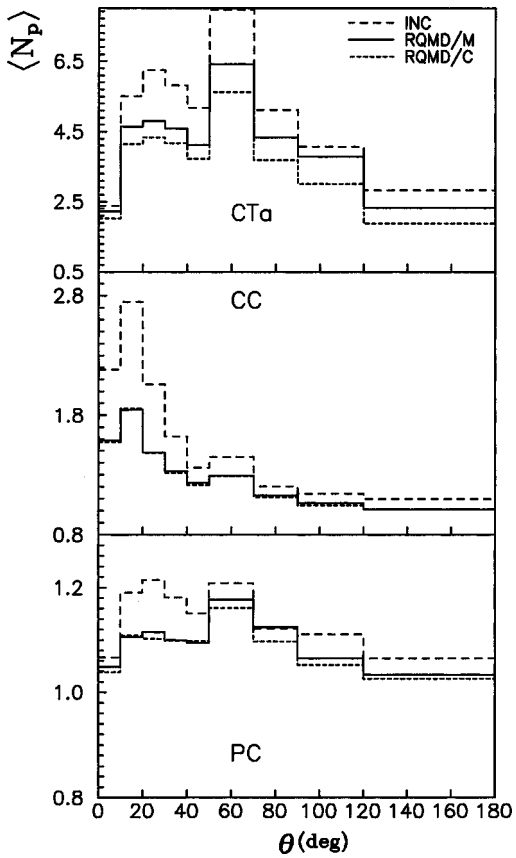

FIG. 4. The calculated mean number of participant protons $\langle N_p \rangle$ as a function of angular interval [θ (deg)] for *p*-C, C-C, and C-Ta interactions. The long-dashed, solid, and small-dashed histograms denote the INC, RQMD/*M*, and RQMD/*C* calculations, respectively.

C-Ta interactions), and thus it results in more $\langle N_p \rangle$. On the other hand, the INC shows more $\langle N_p \rangle$ than both RQMD/*C* and the RQMD/*M* for all studied interactions at all angular intervals. This indicates that the cascade processes built into the INC model are stronger than those predicted by the RQMD model. It is also seen by comparing the RQMD/*M*, RQMD/*C*, and INC results plotted in Fig. 4 with those in Figs. 2 and 3 that the larger the values of $\langle N_p \rangle$, the softer the proton spectrum is. This implies that the measurements do not favor such a large number of participant protons for C-Ta interactions, especially, in the midangular interval.

The difference between the INC and RQMD/*C* results has its reason for the different treatment of the *NN* collision and their time ordering in the two approaches. The *NN* collision times are calculated in the INC [Eq. (3)] in terms of the time coordinate of an observational system common to all nucleons, whereas in the RQMD/*C*, each nucleon has its own eigentime. Consequently, the time ordering of collision events of the former is defined for a given observational frame. Also, the collision criterion in the INC is expressed in terms of the minimum distance in observational frame [Eq. (2)] rather than in the terms of $\sqrt{-q_{Tij}^2}$ defined (in the RQMD) in the *NN* reference system. This unphysical frame dependence in the INC calculations causes, as is also shown in Ref. [11], an unusual excess of the mean number of collisions.

It is interesting to notice that the noninvariance effect becomes significant only when $\langle N_p \rangle \geqslant 2$, which causes a large excess of slow proton spectrum for C-C interactions at $0°-10°$ and a steeper fast proton spectra for C-Ta interactions at $\Delta\theta < 90°-120°$. It is also shown in Ref. [5] that the INC model overestimates the fraction of events with large multiplicities of protons in *AA* interactions at $3.1A-3.5A$ GeV. Therefore, we can conclude that the noninvariance effect is primarily concerned with processes accompanied by a significant destruction of nuclei at the first fast stage of the interaction. This may illustrate that we have to be very careful in applying the INC-type calculations, especially in heavy-ion collisions.

IV. SUMMARY AND CONCLUSION

We have calculated the inclusive proton spectra of *p*-C, C-C, and C-Ta interactions at $3.3A$ GeV as a function of proton kinetic energy (T) in various angular intervals from $0°$ to $180°$ using the RQMD and INC approaches.

First, we have discussed the effect of the mean field on the slow ($T<0.4$) and fast ($T>0.4$) proton spectra. For this purpose, the RQMD code is running in a cascade mode (RQMD/*C*) and including the effect of the mean field (RQMD/*M*). In the case of *p*-C and C-C interactions, there is almost no difference between the RQMD/*M* and RQMD/*C* results for both slow and fast proton spectra at the specified angular intervals; they both agree with the corresponding experimental data. For slow proton spectra in C-Ta interactions, the RQMD/*C* results are in a good agreement with the observed inverse slope parameters (T_B). The introduction of the mean field (RQMD/*M*) has little effect on the T_B values, but gives results in much better agreement with the data. As for the fast proton spectra in C-Ta interactions, both the RQMD/*M* and the RQMD/*C* always underpredict the observed T_B values, while the RQMD/*C* results yield a slightly larger T_B values.

Second, we have investigated the noninvariance effect, caused by the INC calculations, on the slow and fast proton spectra for the interactions under study. This is done by comparing the noncovariant INC with the covariant RQMD/*C* calculations. For the slow proton spectra, the noninvariance effect is observed at $0°-10°$ in *p*-C and C-C interactions, where an unusual excess of slow proton spectra is seen at $T<0.4$ GeV. As for the fast proton spectra, the effect manifests itself in a decrease of the spectra in C-Ta interactions, compared to the RQMD/*C* calculations.

Finally, it is shown that the mean field and noninvariance effects are clearly seen when studying the angular interval dependence on the mean number of participant protons ($\langle N_p \rangle$). Our analysis shows that the noninvariance effect influences both slow and fast proton spectra, whenever the $\langle N_p \rangle$ in the corresponding angular interval exceeds 2.

As the main conclusion of this paper, we would like to emphasize that for the inclusive proton spectra analysis, one cannot use two-body interactions that have no covariant form, especially, in nucleus-nucleus interactions. On the other hand, the disagreement between the RQMD calculations and the experimental fast proton spectra indicates that the key mechanisms of the reaction dynamics are not well determined.

[1] V. S. Barachenkov, Zh. Zhergi, and Zh. Muslamanbekov, JINR Report No. R2-83-117, 1983.

[2] V.D. Toneev and K.K. Gudima, Nucl. Phys. **A400**, 173 (1983); **A401**, 329 (1983).

[3] J. Cugnon, Phys. Rev. C **22**, 1885 (1980).

[4] T. Nishida *et al.*, Report No. JAERI-M-86-116, 1986.

[5] V. Uzhinskii and A.S. Pak, Phys. At. Nucl. **59**, 1064 (1996), and references therein.

[6] J. Cugnon, C. Volant, and S. Vuillier, Nucl. Phys. **A620**, 475 (1997).

[7] E.S. Basova, N.V. Petrov, T.P. Trofimova, and B.P. Tursunov, Phys. At. Nucl. **58**, 223 (1995).

[8] Khaled Abdel-Waged, Phys. Rev. C **59**, 2792 (1999).

[9] Khaled Abdel-Waged, Phys. Rev. C **63**, 024618 (2001).

[10] Kh. Abdel-Waged, A. Abdel-Hafiez, and V.V. Uzhinskii, J. Phys. G **26**, 1105 (2000).

[11] T. Kodama, S.B. Duarte, K.C. Chung, R. Donangelo, and R.A.M.S. Nazareth, Phys. Rev. C **29**, 2146 (1984).

[12] D.E. Kahana, D. Keane, Y. Pang, T. Schlagel, and Shang Wang, Phys. Rev. Lett. **74**, 4404 (1995); J. Zhang *et al.*, Phys. Rev. C **50**, 1617 (1994).

[13] R.K. Puri, E. Lehmann, A. Fassler, and S.W. Huang, Z. Phys. A **351**, 59 (1995); E. Lehmann, R.K. Puri, A. Faessler, G. Batko, and S.W. Huang, Phys. Rev. C **51**, 2113 (1995).

[14] H. Sorge, H. Stocker, and W. Greiner, Ann. Phys. **192**, 266 (1989).

[15] T. Maruyama, S.W. Huang, N. Ohtsuka, G. Li, A. Fassler, and J. Aichelin, Nucl. Phys. **A534**, 720 (1991).

[16] S. Backovic *et al.*, Phys. At. Nucl. **56**, 540 (1993).

[17] G.N. Agakishiev *et al.*, Phys. At. Nucl. **56**, 1397 (1993).

[18] V.S. Barachenkov, K.K. Gudima, and V.D. Toneev, Acta Phys. Pol. **36**, 260 (1969).

[19] V.S. Barachenkov *et al.*, Nucl. Phys. **A187**, 531 (1972).

[20] S. G. Mashnik, in Proceedings of the Specialist Meeting of the Intermediate Energy Nuclear Data: Models and Codes, France, 1994, p. 107.

[21] B. M. Blann, H. Grupprlaar, P. Nagel, and J. Rodens, report, 1994.

[22] Particle Data Group, D. E. Groom *et al.*, Eur. Phys. J. C **15**, 1 (2000).

[23] H. Sorge, R. Mattiello, H. Stocker, and W. Greiner, Phys. Rev. Lett. **68**, 286 (1992); M. Gonin, Ole Hansen, B. Moskowitz, F. Videbaek, H. Sorge, and R. Mattiello, Phys. Rev. C **51**, 310 (1995).

[24] J. Barrette *et al.*, Phys. Rev. C **62**, 024901 (2000).

[25] L. Simic and M. Kornicer, Phys. Rev. C **58**, 2585 (1998).

[26] S. Backovic, I. Picuric, D. Salihagic, D. Krpic, and A.P. Cheplakov, Phys. Rev. C **62**, 064902 (2000).